Combined electromagnetic and photoreaction modeling of CLD-1 photobleaching in polymer microring resonators

Yanyi Huang,[a] Joyce K. S. Poon, Wei Liang, and Amnon Yariv
The Thomas J. Watson, Sr. Laboratories of Applied Physics, California Institute of Technology, Pasadena, California 91125

Cheng Zhang
Center for Materials Research, Norfolk State University, 700 Park Avenue, Norfolk, Virginia 23504

Larry R. Dalton
Department of Chemistry, University of Washington, Box 351700, Seattle, Washington 98195

(Received 14 March 2005; accepted 30 June 2005; published online 9 August 2005)

By combining a solid-state photoreaction model with the modal solutions of an optical waveguide, we simulate the refractive index change due to the photobleaching of CLD-1 chromophores in an amorphous polycarbonate microring resonator. The simulation agrees well with experimental results. The photobleaching quantum efficiency of the CLD-1 chromophores is determined to be 0.65%. The combined modeling of the electromagnetic wave propagation and photoreaction precisely illustrates the spatial and temporal evolution of the optical properties of the polymer material as manifested in the refractive index and their effects on the modal and physical properties of the optical devices. © *2005 American Institute of Physics*. [DOI: 10.1063/1.2031945]

Polymers have been widely used as alternative materials for integrated optical devices in recent years.[1] One of the main advantages of polymer materials is that they can be readily functionalized by incorporating dopant molecules which are photo-, electro-, or chemically active.[2] The physical behavior of devices fabricated from such polymers is thus modifiable by controlling the activity of the dopant molecules. In most studies to date, the properties of the guest/host material are studied independently of the device structure, for example in thin-films, solutions, or bulk powders. Investigations into the mutual dependence of the molecular level interactions and the overall, physical properties of the device will yield insights into precisely how the "macroscopic" optical characteristics of the device are altered by the "microscopic" molecular reactions.

In this letter, we present a combined photoreaction and electromagnetic modeling of the photobleach trimming process of a microring resonator optical filter in amorphous polycarbonate (APC) doped with CLD-1 chromophores (Fig. 1). The photobleaching is modeled with a modified Lambert-Beer's law and a local photoreaction rate equation, which determine the absorption and refractive index profile of the waveguide cross section. Given the refractive index profile, the effective index of the waveguide is computed using a finite-difference (FD) vectorial mode solver. A change in the refractive index due to the photobleaching is reflected in a shift of the microring resonance wavelengths.

The device structure is shown in Fig. 1 and is fabricated using a soft lithographic replica-molding technique.[3,4] The guest-host CLD-1/APC (1:4 weight ratio) serves as the waveguide core, with silica as the lower cladding and air as the upper cladding. The CLD-1 chromophore is originally designed for highly efficient second-order optical nonlinearity due to its strong electron donor-acceptor pair and the rigid ring-locked phenyltetraene conjugated backbone structure.[5] The height and width of the waveguide are 1.6 μm and 1.4 μm, respectively. The microring resonator has a radius of 207 μm. The gap between the ring and the straight waveguide is about 430 nm. For the transmission measurements of the device, the input laser power is set to 100 nW (−40 dBm) to minimize photobleaching of the CLD-1 from the input source. Figure 1 shows the TM-polarization transmission spectrum of the ring resonator filter before photobleaching.

The CLD-1 chromophores are photobleached by focusing broadband visible light from a 100 W halogen lamp with an optical microscope on part of the ring resonator. The exposure intensity is 26 mW/cm^2 over a 0.12 mm^2 area. Figure 2(a) shows the TM transmission spectrum during the photobleaching process, in which the resonance wavelengths

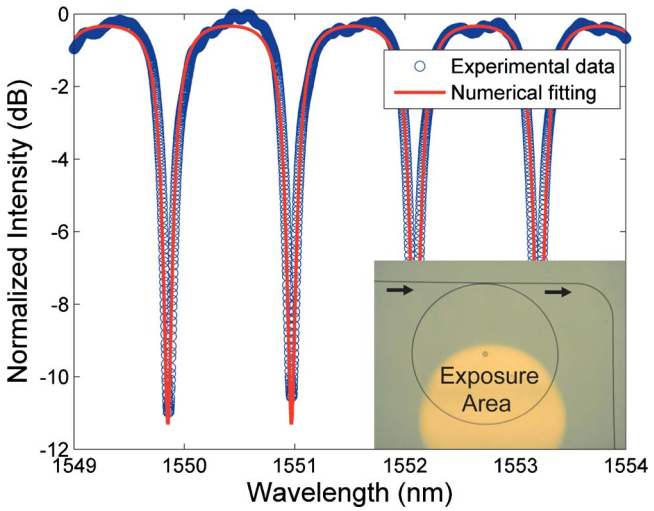

FIG. 1. (Color online). The TM polarization transmission spectrum of a CLD-1/APC polymer microring resonator optical filter around 1550 nm. Inset: An optical microscope photograph of the device. The light green background is the thin residue left from the soft molding. The lighter region is the photobleached area.

[a]Electronic mail: yanyi@caltech.edu

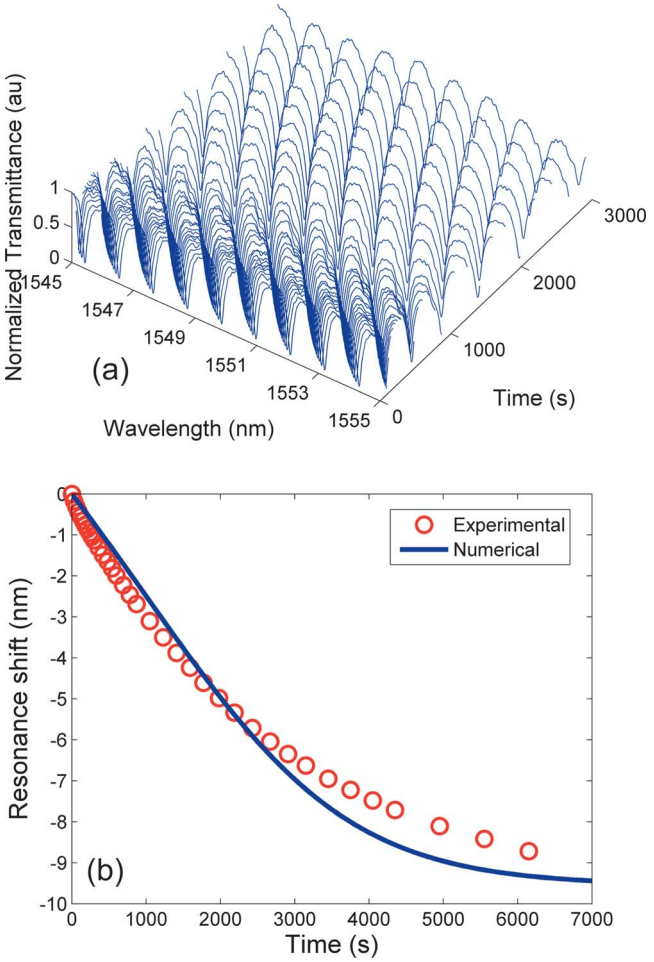

FIG. 2. (Color online). (a) The measured transmission spectra of the CLD-1/APC microring resonator as a function of the photobleaching time. (b) Experimental data (circle) and the numerical fitting (line) using the photoreaction model of the resonance shift as a function of the photobleaching time.

are blueshifted. As shown in Fig. 2(b), the maximum shift of the resonance wavelengths is about −9 nm, indicating that this photobleaching method is highly effective for the post-fabrication trimming of ring resonators.[6,7] In this work, we model the photobleaching process to explain the trend in the observed resonance shift and refractive index change.

To compare the photoreaction modeling with the measured resonance shift, we relate the resonance shift with the effective index (n_{eff}) change,

$$\frac{\Delta\lambda_{\text{res}}}{\lambda_{\text{res}}} = \eta\frac{\Delta n_{\text{eff}}}{n_{\text{eff}}}, \tag{1}$$

where η is the fraction of the ring resonator circumference that is photobleached. Given the waveguide dimensions, n_{eff} is solely determined by the refractive index of the waveguide cross-section. However, n_{eff} cannot be directly obtained from the measured transmission spectrum of the ring resonator primarily due to waveguide dispersion which is dominant over material dispersion in our structures. For a fixed round-trip length, the measured free spectral range (FSR) gives the group index (n_g), not n_{eff}, of the resonator waveguide.[8] However, by determining the waveguide dispersion using a mode-solver, n_{eff} can be extrapolated from n_g, since

$$n_{\text{eff}}(\lambda) = n_g(\lambda) + \lambda\frac{dn_{\text{eff}}(\lambda)}{d\lambda}. \tag{2}$$

In our experiment, η=0.38, the refractive index of APC/CLD-1 is 1.595, and n_g and n_{eff} before the photobleaching are 1.6504 and 1.4814, respectively.

As the CLD-1 is photobleached in the waveguide, the position- and time-dependent change in the concentrations of the unbleached chromophores and bleaching products results in a time-dependent refractive index and absorption gradient in the waveguide. The refractive index at a particular position of the partially bleached CLD-1/APC polymer waveguide can be expressed as[9]

$$n(z,t) = \sqrt{(n_0^2 - n_\infty^2)C(z,t)/C(z,t=0) + n_\infty^2}, \tag{3}$$

where n_0 and n_∞ are the refractive indices of the CLD-1/APC polymer before and after the complete photobleaching respectively, $C(z,t)$ is the concentration of the unbleached CLD-1 chromophore at waveguide depth z at photobleaching time t. z=0 is the top of the waveguide at the polymer/air interface and z=1.6 μm is bottom at the polymer/substrate interface. From the measured transmission spectra, n_0 =1.595 and n_∞=1.568, leaving $C(z,t)$ as the only unknown in Eq. (3). $C(z,t)$ is thus the essential parameter to be determined from the photoreaction model.

The photobleaching of CLD-1 is due to photo-oxidation of the chromophore with singlet oxygen in the presence of an optical excitation.[5,10] In the APC matrix, this process can be regarded as a solid-state photoreaction[11–13] (the glass transition temperature of APC is ~150 °C), in which the reactants and products cannot diffuse. As the bleaching light is illuminated from the top, the reactants closer to the top surface of the waveguide will be bleached faster than those further away. These variations are described by local reaction rate equations to be discussed below.

To model the photobleaching process, we need a relationship between the intensity of the bleaching illumination and the concentration of the reactant. Since the photobleached product is nearly transparent, we model the absorption of the illuminating light with the Lambert-Beer's law[11] and $C(z,t)$ is described by a local photoreaction rate equation. However, since the photobleaching in our demonstration is from a broadband optical source, we introduce a wavelength dependence to the conventional Lambert-Beer's law for monochromatic absorption and the local photoreaction rate equations to arrive at the coupled equations:

$$\frac{dI(z,t,\lambda)}{dz} = -C(z,t)\epsilon(\lambda)I(z,t,\lambda), \tag{4}$$

$$\frac{dC(z,t)}{dt} = -\phi C(z,t)\int \epsilon(\lambda)I(z,t,\lambda)d\lambda, \tag{5}$$

where $\epsilon(\lambda)$ is the molecular absorptivity, z is the depth of the waveguide, $C(z,t)$ is defined in Eq. (3), ϕ is the photobleaching reaction quantum efficiency, and $I(z,t,\lambda)$ is the monochromatic radiation intensity (mole of photons $\text{cm}^{-2}\,\text{s}^{-1}$). To simplify the calculations, we have assumed the photobleaching quantum efficiency is independent of the illumination wavelength. For the initial and boundary conditions of Eqs. (4) and (5), $I(z=0,t=0,\lambda)$ is determined from the measured spectrum of the broadband source and $C(z=0,t=0)$ is known from the weight ratio of CLD-1:APC. The molar absorptivity

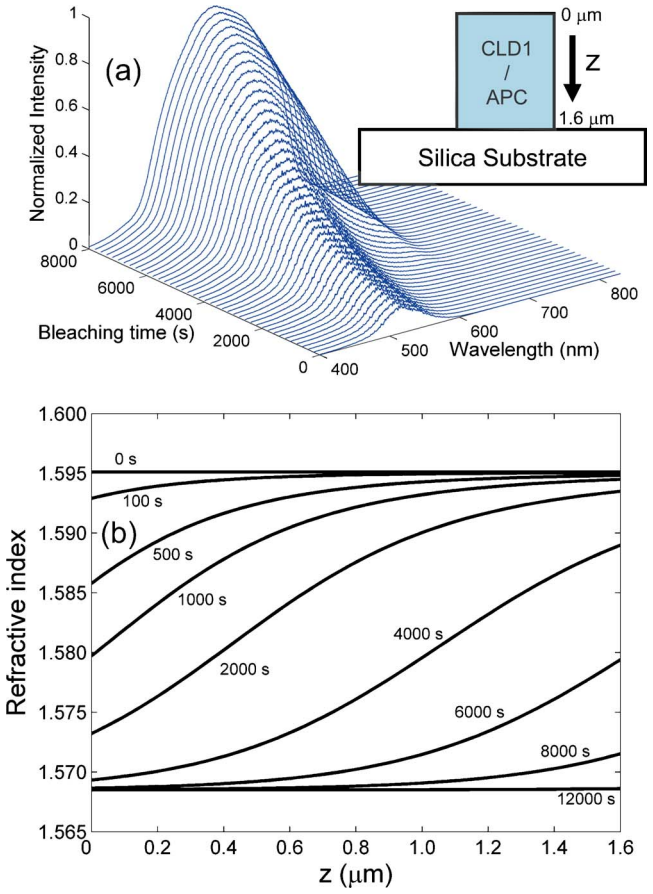

FIG. 3. (Color online). (a) The calculated temporal evolution of the bleaching light spectrum at the base of the waveguide, $z=1.6$ μm. (b) The refractive index profile of the CLD1/APC polymer waveguide at various exposure times.

is extrapolated from the measured absorption spectrum of a CLD-1/APC thin film. Therefore, by solving Eqs. (4) and (5) for a given ϕ, we obtain the light intensity profile, concentration gradient, and hence the refractive index along z.

By combining Eqs. (2)–(5) we fit the theoretical resonance shift as a function of photobleaching time with the experimental result as shown in [Fig. 2(b)]. The fit gives a photobleaching reaction quantum yield of $\phi=0.65\%$. While there is a good agreement between the fit and the measurement, the slight deviation may be due to several factors. First, the actual waveguide cross-section is not exactly rectangular as assumed for the mode calculations, and the base of the waveguide is slightly wider than the top by 0.1 μm. Second, we have not accounted for the photobleaching of the thin ($\sim$40 nm) residue layer from the soft-molding fabrication. Finally, as stated earlier, we have neglected any wavelength dependence in the photobleaching quantum efficiency.

The temporal evolution of the photoreaction [Fig. 3(a)] and refractive index change [Fig. 3(b)], which cannot be determined from the transmission of the ring resonator, is however embodied in Eqs. (3)–(5). The temporal evolution of the material absorption due to the photobleaching is shown in [Fig. 3(a)]. It shows the intensity spectrum at the base of the waveguide ($z=1.6$ μm) as a function of photobleaching time. The broadband illumination spectrum at $z=0$ is eventually recovered as the waveguide is photobleached and becomes more transparent from the top down.

The reactant concentration determined from Eqs. (4) and (5) is substituted into Eq. (3) to yield $n(z,t)$ as in [Fig. 3(b)]. As the refractive index gradient changes in time, the shape of the waveguide mode in the photobleached section is adiabatically modified. Since "macroscopic" quantities such as the effective and group indices completely describe the transmission spectrum of the ring resonator and many other waveguide devices, the detailed index profile and mode shape in the device would not otherwise be known without a consideration of the photoreaction.

In summary, a model of the solid-state photoreaction of the photobleaching of CLD-1 is combined with electromagnetic modal calculations to investigate the observed blueshift in the resonance wavelengths of a CLD-1/APC guest-host microring resonator optical filter. This type of combined modeling is a powerful way of obtaining certain details about the material and device properties which would otherwise be difficult to quantify with conventional optical device characterization techniques.

J.P. is grateful for the support of the Natural Sciences and Engineering Research Council of Canada. The financial support of the National Science Foundation (DMR-0120967), the Defense Advanced Research Projects Agency (N00014-04-1-0094, Dr. D. Honey and Dr. R. Athale), and Hughes Research Laboratories is gratefully acknowledged.

[1] L. Eldada and L. W. Shacklette, IEEE J. Quantum Electron. **6**, 54 (2000).
[2] H. Ma, A. K.-Y. Jen, and L. R. Dalton, Adv. Mater. (Weinheim, Ger.) **14**, 1339 (2002).
[3] Y. Huang, G. T. Paloczi, J. Scheuer, and A. Yariv, Opt. Express **11**, 2452 (2003).
[4] Y. Huang, G. T. Paloczi, A. Yariv, C. Zhang, and L. R. Dalton, J. Phys. Chem. B **108**, 8606 (2004).
[5] C. Zhang, L. R. Dalton, M. C. Oh, H. Zhang, and W. H. Steier, Chem. Mater. **13**, 3043 (2001).
[6] J. K. S. Poon, Y. Huang, G. T. Paloczi, A. Yariv, C. Zhang, and L. R. Dalton, Opt. Lett. **29**, 2584 (2004).
[7] S. Kim, K. Geary, H. R. Fetterman, C. Zhang, C. Wang, and W. H. Steier, Electron. Lett. **39**, 1321 (2003).
[8] P. Rabiei, W. H. Steier, C. Zhang, and L. R. Dalton, J. Lightwave Technol. **20**, 1968 (2002).
[9] C. Gaffney and C. K. Chau, Am. J. Phys. **69**, 821 (2001).
[10] M. E. DeRosa, M. He, J. S. Cites, S. M. Garner, and Y. R. Tang, J. Phys. Chem. B **108**, 8725 (2004).
[11] E. L. Simmons, J. Phys. Chem. **75**, 588 (1971).
[12] J. J. Kim, T. Zyung, and W. Y. Hwang, Appl. Phys. Lett. **64**, 3488 (1994).
[13] J. Vydra, H. Beisinghoff, T. Tschudi, and M. Eich, Appl. Phys. Lett. **69**, 1035 (1996).